Journal of Molecular Neuroscience (2021) 71:2593–2607
https://doi.org/10.1007/s12031-021-01862-2

# miR-128 as a Regulator of Synaptic Properties in 5xFAD Mice Hippocampal Neurons

**Inna Shvarts-Serebro[1] · Anton Sheinin[1] · Irit Gottfried[2] · Lior Adler[1] · Nofar Schottlender[1,2] · Uri Ashery[1,2] · Boaz Barak[1,3]**

Received: 25 March 2021 / Accepted: 25 May 2021 / Published online: 20 June 2021


## Abstract

Alzheimer's disease (AD) is characterized by progressive synaptic dysfunction, deterioration of neuronal transmission, and consequently neuronal death. Although there is no treatment for AD, exposure to enriched environment (EE) in mice, as well as physical and mental activity in human subjects have been shown to have a protective effect by slowing the disease's progression and reducing AD-like cognitive impairment. However, the molecular mechanism of this mitigating effect is still not understood. One of the mechanisms that has recently been shown to be involved in neuronal degeneration is microRNAs (miRNAs) regulation, which act as a post-transcriptional regulators of gene expression. miR-128 has been shown to be significantly altered in individuals with AD and in mice following exposure to EE. Here, we focused on elucidating the possible role of miR-128 in AD pathology and found that miR-128 regulates the expression of two proteins essential for synaptic transmission, SNAP-25, and synaptotagmin1 (Syt1). Clinically relevant, in 5xFAD mouse model for AD, this miRNA's expression was found as downregulated, resembling the alteration found in the hippocampi of individuals with AD. Interestingly, exposing WT mice to EE also resulted in downregulation of miR-128 expression levels, although EE and AD conditions demonstrate opposing effects on neuronal functioning and synaptic plasticity. We also found that miR-128 expression downregulation in primary hippocampal cultures from 5xFAD mice results in increased neuronal network activity and neuronal excitability. Altogether, our findings place miR-128 as a synaptic player that may contribute to synaptic functioning and plasticity through regulation of synaptic protein expression and function.

**Keywords** Alzheimer's disease · miR-128 · SNAP-25 · Synaptotagmin1 · Neuronal activity

## Introduction

Alzheimer's disease (AD) is the most common form of dementia in the elderly and is characterized by progressive cognitive deterioration. AD patients suffer from the impaired ability to form and retrieve memories, deficits in the retrieval of semantic and episodic memories, spatial orientation, and difficulties in language and interpersonal communication (Irvine et al. 2012; Mayeux and Stern 2012). AD pathology is associated with Aβ plaques, tau tangle formation, and cell death in the brain (Terry 2006; Selkoe 2008). These devastating processes are associated with loss of synapses (Selkoe 2008), alterations in synaptic plasticity, and neuronal death that occur in several brain areas including the hippocampus and entorhinal cortex, which are the first to be affected in AD (Masliah et al. 2006; Terry 2006). Furthermore, there is a variety of studies that describe reduced synaptic transmission and decreased synaptic plasticity that worsen with progression of AD pathology (Trinchese et al. 2004; Shankar et al. 2009; Marchetti and Marie 2011; Menkes-Caspi et al. 2015).

While neurodegenerative diseases interrupt normal neuronal functioning and deteriorate cognition, enriched environment (EE) has an opposite effect on synaptic plasticity, neuronal transmission, neuronal viability, and cognitive

✉ Uri Ashery
uriashery@gmail.com

✉ Boaz Barak
boazba@tauex.tau.ac.il

[1] The Sagol School of Neuroscience, Tel Aviv University, Tel Aviv, Israel

[2] The School of Neurobiology, Biochemistry and Biophysics, Faculty of Life Sciences, Tel Aviv University, Tel Aviv, Israel

[3] The School of Psychological Sciences, Tel Aviv University, Tel Aviv, Israel

condition. In humans, individuals who continue to be involved in intellectually stimulating activities maintain higher and prolonged intellectual abilities (Schaie 1993; Eskes et al. 2010), while those with good physical fitness showed improved memory in old age (Chodzko-Zajko et al. 1992).

The effect of EE on AD progression and pathology has been tested in various transgenic mice models of AD and in many cases has been found to have a positive effect on cellular and molecular aspects of the pathology and also on cognition represented by a variety of behavioral tests (Wolf et al. 2006; Costa et al. 2007; Cracchiolo et al. 2007; Beauquis et al. 2013; Balthazar et al. 2018).

Studies of the effect of exposure to EE in rodents revealed changes in expression of many genes that can be linked to neuronal structure, synaptic plasticity, and transmission (Rampon et al. 2000; Frick and Fernandez 2003; Dandi et al. 2018). For example, substantial changes in the expression levels of synaptic proteins, such as the pre-synaptic vesicle protein synaptophysin and postsynaptic density-95 protein (PSD-95) following EE in mice, were presented (Nithianantharajah et al. 2004; Lambert et al. 2005; Liu et al. 2012; Barak et al. 2013; Dandi et al. 2018).

The regulation of these changes at the molecular level and the interplay between these changes and microRNAs′ (miRNAs) regulation have received less consideration. As detailed below, miRNAs act as master regulators of several pathways and have been shown to play a role in several neurodegenerative diseases. In a previous study (Barak et al. 2013), we studied the impact of EE on miRNAs expression in the context of AD pathology. In that study, we performed a comparison between miRNAs that are deregulated in a 3xTg-AD mouse model and those that are altered in mice that were exposed to EE. We found 22 miRNAs inversely regulated in these two groups and suggested that these miRNAs might be involved in the mitigating effect that EE has on AD pathology (Barak et al. 2013).

miRNAs are small non-coding RNAs averaging 22 nucleotides in length, which play a role in a central post-transcriptional regulatory mechanism for gene expression. These RNAs bind the 3′ untranslated region (3′UTR) of mRNA transcripts and facilitate its degradation or inhibit its translation (Bartel 2004; Bushati and Cohen 2008; Shomron et al. 2009; Shomron and Levy 2009). miRNAs are prominent regulators of genes expressed in the brain and are involved in nervous system development, physiology, and disease (Bushati and Cohen 2008). Accumulating evidence indicates that miRNAs play a critical role in the regulation of synaptic activity and plasticity by translational regulation of pre-existing mRNAs in the synapses (Schaefer et al. 2007; Kim et al. 2007; Davis et al. 2008). Furthermore, it has been found that miRNAs also appear to have a fundamental role in various central nervous system (CNS) physio-pathological conditions (Wang et al. 2011; Mouillet-Richard et al. 2012; McNeill et al. 2012; Hu et al. 2017).

miRNAs might contribute to AD's pathogenesis by altering the expression of proteins that influence synaptic plasticity and neuronal transmission or affect cell survival. Several miRNAs that are linked to synaptic plasticity and/or cell survival have been detected as deregulated with the progression of AD in human brains and mouse models (Zovoilis et al. 2011; Wong et al. 2013; Improta-Caria et al. 2020; Vergallo et al. 2021). The Lau et al. (2013) study built a miRNA profile on a large cohort of AD human brains and control group samples. One of the prominent miRNAs in this study is miR-128, the second most significantly deregulated miRNA in human AD patients' hippocampus. This miRNA was also found in our previous study as being significantly downregulated following exposure of C57BL/6 J mice to EE (Barak et al. 2013).

miR-128 is one of the most abundant and highly enriched miRNAs in the adult human and mouse brain (Shao et al. 2010; He et al. 2012). Moreover, expression of miR-128 is the highest in the human brain among the other tissues (Ludwig et al. 2016). miR-128 expression across all brain regions suggests that this miRNA has an important role in processes that are common to many neuronal cell types (Ludwig et al. 2016). Several indications connect miR-128 to neuronal functioning and plasticity. For instance, miR-128 downregulation has been shown to increase cultured cortical network excitability (McSweeney et al. 2016). Moreover, miR-128 has been shown to be involved in regulating motor activity through the regulation of neuronal excitability, and that deficiency of miR-128 in mice resulted in fatal seizures (Tan et al. 2013). Another work presented that miR-128 is essential for fear extinction learning by regulating several genes related to neural plasticity (Lin et al. 2011).

The significant change of miR-128 in AD brains and following EE, together with the indications of its involvement in neuronal plasticity related functions, brought us to investigate how miR-128 affects synaptic proteins and transmission in an AD mouse model.

## Materials and Methods

### Experimented Animals

All experimental procedures were approved by the Tel Aviv University Animal Care Committee (approval 04–17-026), in accordance with the regulations and guidelines of Israel National Institute of Health and the US NIH Guidelines for the Care and Use of Laboratory Animals.

## 5xFAD Model

The 5xFAD model is one of the most early-onset and aggressive amyloid mouse models for AD. It expresses five FAD mutations: human APP with the Swedish (KM670/671NL), Florida (I716V), and London (V717I) mutations, together with mutant presenilin 1 (M146L and L286V) mutations under the control of the murine Thy-1 promotor (Oakly et al. 2006; Ohno et al. 2006).

While the majority of AD transgenic mice form Aβ plaques at ages of 6–12 months or later (Eriksen and Janus 2007), 5xFAD mice start to develop amyloid deposition and gliosis at 2 months and reach a very large burden, especially in the subiculum and deep cortical layers. Intraneuronal Aβ42 accumulates in the 5xFAD brain starting already at 1.5 months of age (before plaques form) and is aggregated within neuron soma and neurites (Oakley et al. 2006). Aβ deposition first emerges in the subiculum of the hippocampal area and layer 5 of the cortex and increases rapidly with age, spreading to fill wide areas of the hippocampus and cortex in 5xFAD mice by the age of 6 months. In contrast to other APP models, where there is no observed neuronal loss, 5xFAD mice develop a severe Aβ deposition with marked synaptic degeneration and neuron loss already by the age of 9 months (Oakley et al. 2006; Ohno et al. 2007).

## Enriched Environment Paradigm

The EE paradigm we used in this study was self-defined by our lab, taking into consideration that the goal of EE is to provide animals with opportunities to express their full range of species-typical behavioral patterns and a certain degree of control over their environment. Our paradigm was designed to avoid aggressive competition between animals and to avoid super-enrichment and stress (Barak et al. 2013). In our enrichment cages, we included running wheels that enable exercise which stimulates neurogenesis (Vivar et al. 2012). In our research, 7-month-old 5xFAD female mice ($n=5$ 5xEE group and $n=5$ 5x-control group) and female 7-month-old WT littermates ($n=5$ wtEE group and $n=4$ wt-control group) mice were exposed to EE or a regular environment for 42 days (8 weeks). The EE cages were equipped with two running wheels for spontaneous exercise. Every 10 days, the bedding and nesting material, a house, and toys were changed. The control group of mice was housed in smaller, regular cages without running wheels, toys, or any stimulating objects, with 5–6 mice per cage, as in the EE group.

## RNA Extraction

For the miRNA profiling by TaqMan low-density arrays, the total RNA was extracted from the whole hippocampi of mice using TRIzol reagent (Invitrogen, USA).

For miRNA levels quantification by qRT-PCR, the total RNA was extracted from the whole hippocampi of mice using mirVana™ PARIS™ RNA Kit. The final RNA concentration and purity were measured using a NanoDrop ND-1000 spectrophotometer (NanoDrop Technologies, Thermo Scientific, USA).

## Quantitative RT-PCR

For qRT-PCR analysis of mature miR-128, 2.5 µl of 4 ng/µl total RNA were used for the synthesis of the first-strand cDNA using a MultiScribe reverse transcriptase reaction with the High Capacity cDNA kit (Applied Biosystems, USA) and TaqMan MicroRNA Assay RT primer (Applied Biosystems) for each miRNA.

Mixtures containing cDNA, RNase-free water, and TaqMan MiRNA Assay Real-Time probe (Applied Biosystems) for each miRNA were loaded on a 96-well plate.

The PCR amplification reaction was carried out using Applied Biosystems 7300 Fast Real-Time PCR System under the following thermal cycler conditions: 2 min at 50 °C, 20 s at 95 °C, 40 cycles of (3 s at 95 °C and 30s at 60 °C).

The expression of tested mature miRNAs was normalized to the expression of U6 snRNA, and the relative quantification method, $2^{-\Delta\Delta Ct}$, was used to calculate the expression relatively to the mean of the U6 snRNA.

## Immunofluorescence Staining

The brain hemispheres were fixed overnight with 4% paraformaldehyde in 0.1 M phosphate buffer (pH 7.4) and then placed in 30% sucrose for 48 h. Thirty micrometer coronal sections were prepared by cutting the frozen hemispheres on a sliding microtome. The slices were serially collected and stored in cryoprotectant (containing glycerin, ethylene glycol, and 0.1 M sodium phosphate buffer, pH 7.4) at − 20 °C until use. For staining, free-floating coronal sections were washed in PBS to remove any remnants of the cryoprotectant solution. For better antigen retrieval in Aβ staining, before blocking, the slices were incubated for 6 min in 70% formic acid and washed in PBS. Sections were blocked with 20% normal goat serum (Vector Laboratories, Burlingame, CA, USA) with 0.1% Triton X-100 for 2 h at RT. Then, the sections were incubated with biotinylated mouse anti-Aβ 17–24 (4G8, 1:200; Signet Laboratories) for 1 night at 4 °C. After rinsing with PBST (PBS with 0.1% Triton X-100), the sections were incubated for 1 h at RT in a 1:1000 dilution in 2% normal goat serum in PBST with anti-mouse 568 (Alexa Fluor, Invitrogen, Carlsbad, CA, USA) secondary antibody. Then, the sections were rinsed again with PBST and mounted on a slide sealed with a coverslip. To minimize

variability, sections from all animals were stained and treated simultaneously.

## 3′UTR Constructs for the Luciferase Assay

Fragments of *SNAP-25*, synaptotagmin-1 (*Syt-1*), and *Ppp1cc* 3′UTRs that include binding sites for miR-128 were cloned into psiCHECK™-2 plasmid (Promega, USA) downstream to the Renilla Luciferase Reporter gene, into XhoI–NotI restriction sites. Firefly luciferase reporter, which is part of the psiCHECK™-2 plasmid, serves as an internal control (under a different promoter). The 3′UTR fragments were PCR-amplified from mice tail DNA and XhoI–NotI restriction sites were added (restriction sites are in lower case italics).

*SNAP-25*: 3′UTR length is 868 bp — includes 2 binding sites for miR-128. The primers that were used for this purpose:
*SNAP-25*-Fwd: CCA*ctcgag*GAGGGTCATTGTGTGACA TC.
*SNAP-25*-Rev: GGT*gcggccgc*GGAGGGATTTAATAT ACATGC.
*Syt1*: 3′UTR length is 445bp — includes 2 binding sites for miR-128. The primers that were used for this purpose:
*Syt1*-Fwd: CCA*ctcgag*GCAACCTCTTATGTACACTAG.
*Syt1*-Rev: GGT*gcggccgc*GAAGCAGTGTTAGGTAGC AG.
*Ppp1cc*: 3′UTR length is 483bp — includes 1 binding site for miR-128. The primers that were used for this purpose:
*Ppp1cc*-Fwd: CCA*ctcgag*GTGATGTGCTGGTCAGCT TG.
*Ppp1cc*-Rev: GGT*gcggccgc*CTTCAGATAGTCTGG GCAGGG.

As a control for the specific binding of a selected miRNA to its binding sites in relevant 3′UTR, a scrambling of miR-128 seed binding sites in the 3′UTR was performed by mutagenesis. The mutagenesis was carried out by PCR reaction of the plasmid using the enzyme Phusion DNA Polymerase (Thermo Scientific, USA) with GC buffer. PCR reaction conditions: (1) 98 °C for 2 min, (2) (98 °C for 30 s, 55 °C for 30 s, 72 °C for 30 s/kb) X18, and (3) 72 °C for 10 min.

Since *SNAP-25* and *Syt1* 3′UTRs include 2 binding sites for miR-128, the scrambling of both binding sites was performed with 2 different mutagenesis primers.

The primers that were used for mutagenesis are (the scrambled seed site is in lower case italics):

*SNAP-25*-miR-128-location1-Fwd: GTATTGTTCTTG TAAA*ctcagag*CATTCCACAGAGCTAC.
*SNAP-25*-miR-128-location2-Fwd: GAAAATATAGAT AA*ctcagag*GATAAATATCATTAC. miR-128 seed sites in SNAP-25 3′ UTR: ACTGTGA.
*Syt1*-miR-128-location1-Fwd: GACTGCTCTGTG TAAC*ctcagag*CTGCCCTGTGTGCTTAG.
*Syt1*-miR-128-location2-Fwd: CAGCATCTTGTCAAC *ctcagag*CTAGTCCACATTTGTC.
miR-128seed sites in SYT1 3′ UTR: CACTGTG.

After digesting the methylated source plasmid with DPN1 (New England Biolabs, UK), the mutated plasmid was sequenced to verify that the desired mutagenesis was achieved and that no additional unexpected mutations were created.

## miR-128 Overexpression Construct for Luciferase Assay

The pre-miRNA of miR-128 was cloned into the XhoI–NotI restriction sites of the PLL3.7 lentiviral vector. For this purpose, a DNA fragment of ~110 bp upstream and downstream of the pre-miRNA was PCR-amplified from mice tail DNA and XhoI and NotI restriction sites were added (restriction sites are in lower case italics). The primers that were used for this purpose:

miR-128-Fwd: ACG*ctcgag*CTTGAAAGAAATGGA CCAAG.
miR-128-Rev: GTA*gcggccgc*GTATGAAGCCAAGGT TGTTAC.

## Dual Luciferase Assay

HEK293T cells were seeded in 24-well plates in DMEM, supplemented with 10% FBS and 1% Pen-Strep. The cells were transfected 24 h after seeding with 485 ng PLL3.7 containing the pre-miR-128 or an empty vector and 5ng psiCHECK™-2 containing the desired 3′UTR with or without site-directed mutations. The transfection was done using the JetPEI Transfection Reagent (Polyplus Transfection), according to the manufacturer's protocol.

Firefly and Renilla luciferase activities were measured 48 h after transfection using the Dual-Luciferase Reporter Assay System kit (Promega, USA) and a Veritas microplate luminometer (Promega), according to Promega's protocol. The assay was conducted after verification of > 50% transfection efficiency, as was measured by GFP fluorescence.

## Hippocampal Primary Neuronal Culture

The protocols of this experiment were approved by the Institutional Animal Care and Use Committee of the Tel Aviv University. The primary hippocampal neuronal cultures were prepared from newborn P0-P2 5xFAD mice. The hippocampal tissue was separated from the cortex, incubated for 15 min with papain (100 U, Sigma-Aldrich, St. Louis, MO, USA) in $Ca^{2+}$/$Mg^{2+}$-free Hank's balanced salt solution (HBSS) (Biological Industries, Israel), and then, it was mechanically dissociated. The cells were plated, in a modified essential medium (MEM) without L-glutamine, with essential amino acids (Biological Industries, Israel), 5% heat-inactivated fetal calf serum (FCS, Biological Industries, Israel) to support glial cell growth, heat-inactivated 5% horse serum (Biological Industries, Israel), 2 mM glutamine (Biological Industries, Israel), 3 mg/ml glucose (Sigma-Aldrich), 2% B-27 (Gibco), and 0.5% Pen-Strep (100 U/ml penicillin, 100 µg/ml streptomycin; Biological Industries, Israel).

The cells were plated on 18-mm glass coverslips pre-treated with polyethylenimine (PEI, 1:5000, Sigma-Aldrich) to promote neuronal adhesion. The plating density of the cells was 2000–2500 cells/$mm^2$ (~$6 \times 10^5$ cells per dish) for calcium imaging and 2500–3000 cells/$mm^2$ (~$10^6$ cells per dish) for western blot analysis. The cultures were maintained at 37 °C with 5% $CO_2$. On the following day and every 3–4 days thereafter, the medium was exchanged with growth medium, which was essentially the plating medium but without the FCS.

## Western Blotting

Primary neuronal cultures were infected at 7 DIV with a Lentivirus carrying sponge construct of miR-128 (miR128-Sp) or with control construct that is missing the active miR-128 sponge sequence. At 21 DIV, the proteins were extracted by a solubilization buffer and dissolved in a lysis buffer containing: 7.5 mM HEPES pH7, 1.5 mM EDTA, 1.5 mM EGTA, 0.375 mM DTT, protease inhibitor cocktail (P8340; Sigma-Aldrich), phosphatase inhibitor cocktail (P5726; Sigma-Aldrich), and 25% of 10% SDS (Amresco Pure, Technology Grade). Protein concentrations were determined using the Bradford assay (Bio-Rad). The protein extracts (~40 µg protein) were run on an SDS–polyacrylamide (10%) gel and then transferred to a nitrocellulose membrane by electroblotting.

The membranes were blocked overnight in 5% (weight/volume) non-fat milk in 0.1% Tween 20 Tris-buffered saline (TBS). After the blocking, the membranes were incubated for 1 h at room temperature with primary antibodies: rabbit anti-SNAP-25 (1:1000, 111,002, Synaptic Systems), rabbit anti-synaptotagmin-1 (Syt1, 1:1000, 105,102, Synaptic Systems), and mouse anti-clathrin heavy chain (CHC, 1:1000, C1860, Sigma-Aldrich).

The membranes were then washed in Tween 20-TBS for 20 min and incubated at room temperature with specific horseradish peroxidase-conjugated secondary antibodies at a dilution of 1:15,000 (Jackson ImmunoResearch Laboratories) for 60 min. The immunoblot bands were developed using an enhanced chemiluminescent substrate (Pierce), and their intensities were quantified with ImageQuant TL (Amersham). CHC protein levels were used to verify uniform loading of the samples across the gel and for quantification normalization of the examined protein expression levels.

## Calcium Imaging

Hippocampal primary cultures were infected at 7 DIV with a Lentivirus carrying miR128-Sp or a control construct that is missing the active miR-128 sponge sequence. Both miR128-Sp and control constructs included a GFP expressing sequence under human Synapsin promoter (hSyn-GFP). We also infected the cultures with an AAV virus that expresses the CAR-GECO red $Ca^{+2}$ sensor, which increases its fluorescence upon elevation of intracellular $Ca^{2+}$ concentration. The activity of the neuronal network was recorded at 21 DIV in an open-air environment. The culture medium was replaced by Tyrode's solution containing 120 mM NaCl, 2.5 mM KCl, 2 mM $CaCl_2$, 2 mM $MgCl_2$, 25 mM HEPES, and 30 mM glucose. Prior to the recordings, the cultures were incubated for 30 min in Tyrodes for stabilization and were kept at 37 °C. The recordings were performed with an iMIC inverted microscope fitted with an EMCCD camera (Andor DU 888D) and a 20× air objective (Olympus, 20X 0.5 NA).

The imaging of GFP expressing neurons was performed using a 491 nm wavelength laser to select only the miR128-Sp or its control expressing neurons for $Ca^{+2}$ imaging recordings. Using a 561-wavelength laser, we recorded spontaneous neuronal activity in the chosen neurons that were represented by elevation in fluorescence intensity of the CAR-GECO red calcium sensor with the increase in intracellular calcium concentration as a representative for action potentials evoked in neurons. The equipment was controlled by Live Acquisition Software (TILL Photonics). The data for analysis was collected by an "online kinetics" program and was analyzed using a self-developed Microsoft Excel macro.

## Electrophysiology

Hippocampal primary cultures were infected at 2 DIV with a lentivirus carrying miR128-Sp or a control construct that is missing the active miR-128 sponge sequence. Both the miR-128Sp and the control constructs included a GFP expressing sequence under a human synapsin promoter (hSyn-GFP). Current clamp recordings were performed at

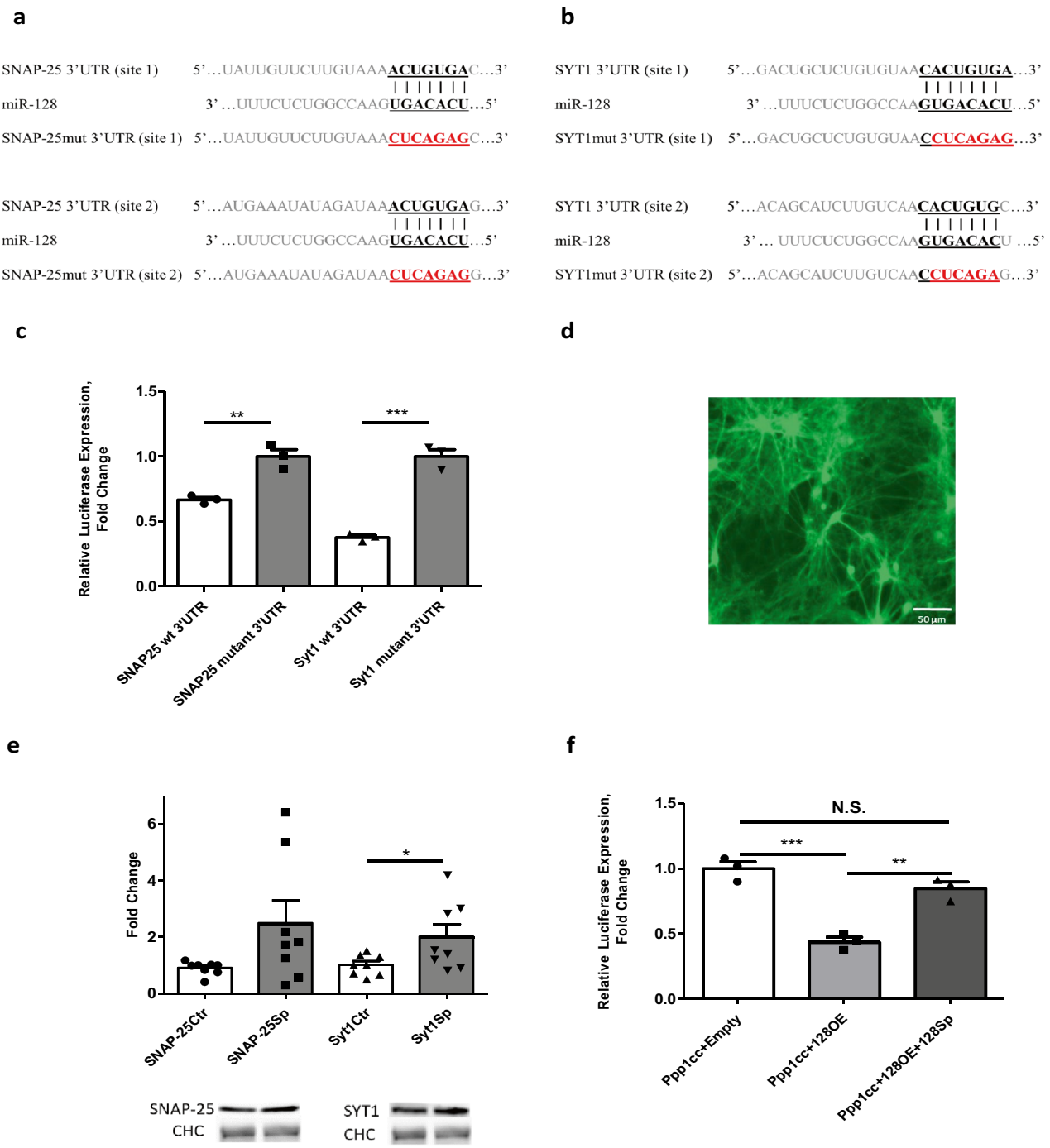


14 DIV utilizing EPC-10 patch-clamp amplifier and Patchmaster software (HEKA Electronics Gmbh, Lambrecht, Germany). The extracellular solution consisted of 140 mM NaCl, 3 mM KCl, 2 mM $CaCl_2$, 1 mM $MgCl_2$, and 10 mM HEPES (Sigma-Aldrich), supplemented with 2 mg/ml glucose (Sigma-Aldrich), pH 7.4, osmolarity adjusted to 300–305 mOsm. The patch pipettes had resistances of 3–5 MOhm after filling them with a solution containing 135 mM KCl, 10 mM HEPES, 5 mM glucose, 1 mM $K_2ATP$, and 1 mM MgATP (Sigma-Aldrich), pH 7.4, osmolarity adjusted to 285–290 mOsm. In order to evoke a single action potential and assess its parameters, we used 5-ms duration square current pulses of varying intensity that were injected into the cells. In order to measure the rheobase and assess the repetitive firing, long (500 ms) depolarization current steps of varying intensity (50–500 pA) were injected. Signals were filtered at 2 kHz and sampled at 5 kHz. The data were analyzed with Igor Pro software

◂**Fig. 1** miR-128 directly binds *SNAP-25* and *Syt1* mRNA and regulates SNAP-25 and Syt1 protein expression. Bioinformatics analysis (using Targetscan) of miR-128′ predicted targets revealed two binding sites for miR-128 in *SNAP-25* and *Syt1* mRNAs' 3′UTR. For verification of miR-128's direct regulation of *SNAP-25* and *Syt1* mRNAs, using luciferase assay, we created constructs that contains intact or mutated miR-128 binding sites in **a** *SNAP-25* and **b** *Syt1* 3′UTRs. The mutations were created by scrambling the nucleotides (shown in red) in the seed regions of miR-128's target sites. **c** Luciferase assay demonstrates *SNAP-25* and *Syt1* mRNA targeting by miR-128. miR-128 reduced the expression of Firefly luciferase fused to 3′UTR of *SNAP-25* by 35% and *Syt1* by 64%, indicating a direct regulation of SNAP-25 and Syt1 protein expression by miR-128. **d** Primary whole-brain neuronal cultures of 5xFAD mice were infected with miR128-Sp or with the control construct (miR128-Ctr) to investigate the effect of this miRNA on SNAP-25 and Syt1 protein expression. GFP expression in the infected neurons reveals around 90% infection rate of both. **e** Western blot analysis of 5xFAD primary cultures 14 days after infection revealed that miR-128 affects both SNAP-25 and Syt1 proteins and their expression levels increased in cultures in which miR-128 expression was downregulated (SNAP-25Sp and Syt1Sp), in comparison to control cultures that are missing the active area of the sponge (SNAP-25Ctr and Syt1Ctr). The quantification was done upon normalization to CHC housekeeping gene expression. **f** miR-128 sponge (128Sp) functionality verification. Cotransfection of the Ppp1cc-luciferase (*Ppp1cc*) construct with an empty vector resulted in basal luciferase activity representing expression of Ppp1cc-luciferase. Overexpression of miR-128 (128OE) cotransfected with Ppp1cc-luciferase construct, led to decreased Firefly luciferase activity. Cotransfection of miR128-OE together with miR128-Sp and Ppp1cc-luciferase construct abolished the effect of miR128-OE on luciferase activity, measured as the basal level (empty vector only). The results are presented as mean + SEM ($n = 3$ in **a**, **d**; $n = 8$ in **c**). Statistical significance was assessed by Student's unpaired *t*-test in **a** and **c**, and by one-way ANOVA with Bonferroni multiple comparison test in **d**.*$p < 0.05$; **$p < 0.01$; ***$p < 0.001$. N.S., non-significant difference

(Wavemetrics, Lake Oswego, OR, USA) and custom-written macros.

## Results

### miR-128 Regulates SNAP-25 and Syt1 Protein Expression

We were first interested in defining potential mRNAs that are predicted to be regulated by miR-128. Searching the Targetscan v7.2 tool (http://www.targetscan.org), a bioinformatical prediction algorithm that defines the genes that may possibly be targeted by a specific miRNA, revealed that among the various targets, miR-128 is predicted to regulate mRNAs that code for two key synaptic proteins: SNAP-25 and Syt1. These proteins play an essential role in vesicular release and synaptic transmission (Sutton et al. 1998; Washbourne et al. 2002; Sudhof 2004; Choi, 2010; Mohrmann et al. 2015; Wang et al. 2016; Zhou et al. 2017). Since neuronal activity and synaptic transmission are dramatically impaired in AD, we were highly interested in investigating the effect of miR-128 on neuronal functions and whether it directly regulates the expression of SNAP-25 and Syt1 by binding to their mRNAs.

In order to determine whether miR-128 directly binds to the 3′UTR of these putative target genes, we performed dual-luciferase reporter assay using HEK293T cells. The 3′UTR fragments of *SNAP-25* and *Syt1* mRNAs, which both contain two miR-128 binding sites with or without these sites' directed mutation (Fig. 1a, b), were cloned upstream to a Firefly luciferase reporter. Overexpression of miR-128 together with the vector expressing luciferase fused to *SNAP-25* and *Syt1* 3′UTR led to a reduction of 35% and 64%, respectively, in luciferase activity (Fig. 1c) compared to the constructs where binding of miR-128 to the 3′UTR was interrupted due to miR-128 binding site directed mutation. These results show that miR-128 directly binds to the mRNAs of *SNAP-25* and *Syt1* and directly regulates their expression.

To further validate the interaction between miR-128 and these synaptic proteins, we investigated the impact of miR-128 downregulation on SNAP-25 and Syt1 proteins expression levels in neurons. For this purpose, we downregulated miR-128 expression in primary neuronal cultures using miR-128 sponge (miR128-Sp) construct that was kindly provided by Prof. Timothy W. Bready (Queensland Brain Institute, Australia) (Lin et al. 2011). We infected primary neuronal cultures from 5xFAD mice with lentivirus expressing miR128-Sp or with control construct that is missing the active sequence of the miR-128 sponge at 7 DIV. The constructs also expressed GFP to verify infection efficiency. The infection rate of both constructs was around 90% (Fig. 1d). At 21 DIV, we extracted the proteins from the cells and quantified the expression levels of SNAP-25 and Syt1 using western blot analysis. We hypothesized that downregulation of miR-128 would result in an increase in the expression levels of its targets. As shown in Fig. 1e, both SNAP-25 and Syt1 proteins levels were increased due to miR-128 downregulation — findings that are strengthening the role of miR-128 in the regulation of the expression of these two key proteins in synaptic transmission.

To verify the downregulation capability of the sponge construct we have used, we performed a dual luciferase reporter assay. To do so, we cloned the 3′UTR fragment of *Ppp1cc* mRNA, which is a verified target of miR-128 (Lin et al. 2011), upstream to the Firefly reporter mRNA (Ppp-Luc) and expressed it alone (with an empty vector) or cotransfected it with miR128-OE (overexpression of miR-128). We hypothesized that cotransfection of miR128-OE and Ppp-Luc would reduce Firefly luciferase expression due to binding of the overexpressed miR-128 to the *Ppp1cc* 3′UTR fused to the Firefly reporter mRNA, thus reducing the translation of the luciferase protein. Indeed, cotransfection of miR128-OE and Ppp-Luc constructs

resulted in decreased activity of the firefly luciferase compared to the basal luciferase activity that was measured when we cotransfected Ppp-Luc construct with an empty vector. Then we used this system to also assess the ability of miR128-Sp to downregulate miR-128 activity. Cotransfection of miR128-OE together with miR128-Sp and Ppp-Luc construct abolished the effect of miR128-OE on luciferase activity, resulting in luciferase activity levels similar to those measured when transfecting with empty vector only (Fig. 1f), proving the efficiency of miR128-Sp in downregulation of miR-128 expression.

## miR-128 Expression is Being Downreguated in 5xFAD Mice with the Progression of AD Pathology

Next, we were interested to study miR-128's levels in a mouse model of AD during different stages of the disease progression. For this purpose, we chose the 5xFAD mouse model, in which the AD phathology is being rapidly developed, and amyloid deposits are visible as early as at ~ 2 months of age (Oakley et al. 2006). We first examined whether miR-128 expression is being altered in 5xFAD mice compared to controls, and whether its alteration matches the findings from individuals with AD (Lau et al. 2013).

We used qRT-PCR method to examine the changes in the expression levels of miR-128 in the hippocampi of 5xFAD mice along the progression of AD pathology in 3 different ages, representing different phases in the severity of AD pathology: 2 months of age (initial AD pathology), 8 months of age (severe pathology), and 12 months of age (chronic severe AD pathology). Immunohistochemical staining of Aβ plaques in the hippocampi of 5xFAD mice presents an increase in plaques burden across the selected ages that correlates with the progression of AD pathology (Fig. 2a). Interestingly, we found that at the initial stages of the disease (2 months of age), there is no significant change in the expression levels of miR-128 in 5xFAD mice compared to their WT littermates (Fig. 2b). At 8 months of age, when the pathology is progressive, and Aβ plaques are already spread across the hippocampal area (Kimura and Ohno 2009), the expression level of miR-128 is significantly downregulated in the hippocampi of 5xFAD mice compared to WT littermates (Fig. 2a, b). These findings resemble the changes reported for this miRNA in individuals with AD (Lau et al. 2013) and therefore place the 5xFAD mouse as a suitable model for investigating miR-128 role in AD pathology. In 12 months of age, the difference in miR-128 levels between the 5xFAD and WT littermates' hippocampi is diminished and becomes insignificant (Fig. 2b).

## miR-128 Expression is Being Downreguated in WT, but Not in 5xFAD Mice Exposed to EE

Following our previous finding that EE downregulates miR-128 expression in WT mice (Barak et al. 2013), we were interested in investigating whether the exposure to an EE, which has been shown to increase plasticity in the hippocampus, would have the same effect on 5xFAD mice.

Since we found a significant reduction in miR-128 levels in 8-month-old 5xFAD mice compared to controls (Fig. 2b), we looked for changes in this miRNA's expression level following EE, at the same age of mice (8 months old). In this experiment, we exposed 7-month-old 5xFAD mice and their WT littermates for 42 days to an EE (Barak et al. 2013). We had four experimental groups: WT and 5xFAD groups that were exposed to EE (labeled as wtEE and 5xEE) and their control WT and 5xFAD littermates that were accommodated in regular cages (labeled as wtCtr and 5xCtr). At the end of the EE period, at the age of ~ 8.5 months, we performed qRT-PCR analysis and quantified the hippocampal levels of miR-128 in the different experimental groups.

We found that WT mice showed significant downregulation of miR-128 expression levels following EE (Fig. 2c). Interestingly, in 5xFAD mice, EE did not significantly affect the expression levels of miR-128.

## miR-128 Downregulation Increases Neuronal Activity in Hippocampal Primary Cultures Derived from 5xFAD Mice

Next, we turned to examine whether downregulation of miR-128 indeed affects neuronal connectivity and activity, as expected from its regulation of Syt1 and SNAP-25 protein level expression in neurons derived from 5xFAD mice. For this purpose, we chose to work with 5xFAD hippocampal primary neuronal cultures to investigate whether downregulation of miR-128 expression levels would increase neuronal network activity in this model.

To address this, we utilized the calcium imaging technique. We measured the calcium bursting activity as a readout of neuronal activity of 5xFAD hippocampal primary cultures infected with lentivirus expressing miR128-Sp (5xSp) or a control construct missing the sponge's active area (5xCtr). All the cultures were also infected with AAV virus transducing CAR-GECO red, a $Ca^{2+}$ sensor that increases its fluorescence upon elevation of intracellular $Ca^{2+}$ concentration (Fig. 3a). The cultures were infected at 7 DIV, and the neuronal network activity was recorded at 21 DIV. The network activity was synchronous both in 5xSp and in 5xCtr experimental groups (Fig. 3b, c). The 5xFAD primary cultures infected with miR-128 sponge (5xSp) showed significantly higher network activity represented by increased

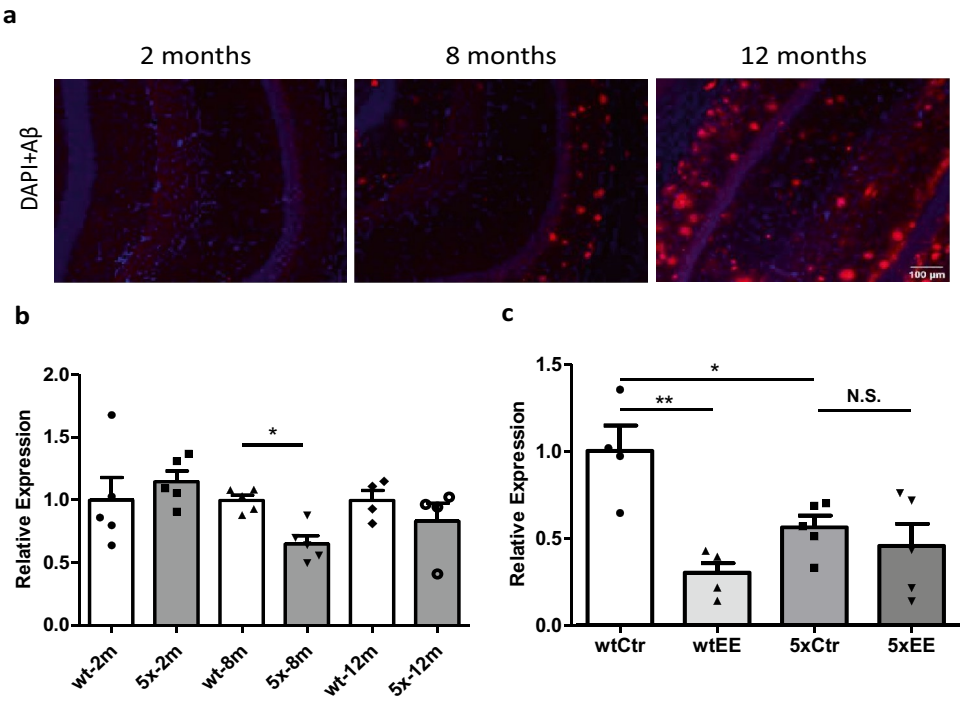


**Fig. 2** miR-128 is being downregulated following the progression of AD pathology in 5xFAD mice and following EE in WT but not in 5xFAD mice littermates. **a** Representative immunohistochemical staining for Aβ in the hippocampus of 5xFAD mice presents the differences in Aβ plaque loads at 2, 8 and 12 months of age. **b** qRT-PCR assay was utilized to quantify expression levels of miR-128 in the hippocampal area of 5xFAD mice along the progression of AD pathology, compared to age-matched WT littermates. The levels of miR-128 were measured in initial (2-months-old), progressive (8-months-old) and severe (12-months-old) stages of AD pathology in this model. In the initial pathology stage, there is no significant difference in miR-128 expression level compared to WT. In 8-month-old 5xFAD mice, miR-128 levels are significantly downregulated compared to WT, and this trend is conserved also in 12 months of age, although not statistically significant. **c** The levels of miR-128 in the hippocampal area of 8.5-month-old 5xFAD and their WT littermates with and without exposure to EE. miR-128 levels are significantly downregulated in 5xCtr mice in comparison to wtCtr littermates. In WT mice groups, miR-128 levels are significantly downregulated following exposure to EE, while in 5xFAD there is no significant effect of the exposure to EE on the expression levels of miR-128. wt, WT mice; 5x, 5xFAD mice; wtCtr, WT mice in regular cages (no EE); wtEE, WT mice exposed to EE; 5xCtr, 5xFAD mice in regular cages (no EE); 5xEE, 5xFAD mice exposed to EE; N.S. non-significant difference. Results presented as mean + SEM. Statistical significance was assessed by Student's unpaired *t*-test in **a**, and by two-way ANOVA with Student's unpaired multiple comparison *t*-test in **b**. $^{*}p < 0.05$; $^{**}p < 0.01$; $n = 4–5$

synchronous spiking rate: an average of 13.98 (SEM = 4.127; $n = 5$) calcium bursts in 5 min in 5xSp cultures, in comparison to an average number of 4.2 (SEM = 0.5132; $n = 6$) calcium bursts in 5 min in 5xCtr cultures (Fig. 3b, c, and d). Accordingly, inter-spike interval was significantly lower in 5xSp cultures (average interval of 0.54 s s ± 0.1759 SEM; $n = 5$) in comparison to the 5xCtr cultures (average interval of 1.725 s ± 0.3467 SEM; $n = 6$) (Fig. 3e). The higher bursting activity may result from elevated levels of the synaptic proteins Syt1 and SNAP-25 that enhance synaptic transmission.

## miR-128 Downregulation Increases Neuronal Excitability

Finally, we performed whole-cell patch-clamp recordings to examine whether miR-128 expression levels also impact the intrinsic neuronal excitability. The recordings were done at 14 DIV from 5xFAD hippocampal primary neurons with reduced miR-128 expression levels (5xSp) compared to 5xFAD control cultures (5xCtr). We measured the minimal current required to evoke an action potential by step wise increasing the stimulation voltage as an estimate for the rheobase. The rheobase test showed that in 5xFAD neurons expressing miR128-Sp, lower voltage can elicit an action potential suggesting that these cells are more excitable than those that are expressing control construct (Fig. 4a, b). Also, the number of action potentials evoked in a certain current was higher in 5xSp cultures in comparison to their control (5xCtr) (Fig. 4c). Last, the rate of the falling phase of the action potentials (Fig. 4d) was faster in neurons with reduced levels of miR-128 than in control neurons. These results suggest that downregulating miR-128 expression elevates neuronal excitability, which can also contribute to the increased neuronal network activity demonstrated in Fig. 3.

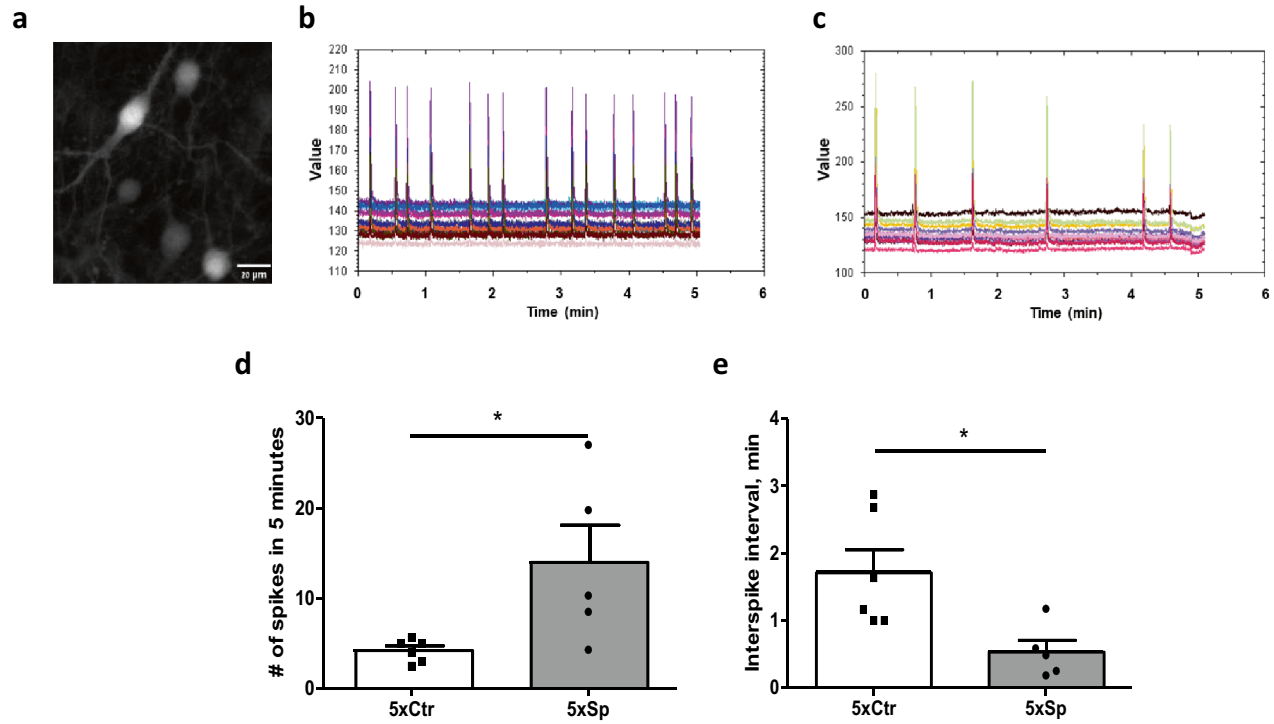


**Fig. 3** miR-128 downregulation increases neuronal network activity in primary hippocampal cultures of 5xFAD mice. 5xFAD hippocampal primary neuronal cultures were infected with miR-128-Sp (5xSp) or with a control construct missing the active sponge sequence (5xCtr) together with CAR-GECO red as a $Ca^{2+}$ sensor. **a** Representative neurons expressing CAR-GECO to monitor calcium bursting as a mean for neuronal activity. **b** Representative activity of single neurons measured as changes in the fluorescence intensity of CAR-GECO red showed enhanced calcium burst activity following miR-128 sponge-expression compared to **c** control (**b**, **c** — each color represent a different neuron). Cultures infected with miR128-Sp showed **d** increased spiking rate and **e** reduced inter-spike interval compared to control cultures. The results are presented as mean + SEM ($n = 5–6$). Statistical significance was assessed by Student's unpaired *t*-test. $*p < 0.05$

## Discussion

Our research shows that miR-128 is a regulator of two central proteins in synaptic transmission machinery: SNAP-25 and Syt1 (Mohrmann et al. 2013; Ashery et al. 2014; Rizo and Xu 2015; Brunger et al. 2019).

Syt1 is a calcium sensor that triggers vesicle fusion as a response to calcium influx following an action potential in a synapse (Katz and Melidi 1970; Brose et al. 1992; Zhou et al. 2017), whereas SNAP-25 has a central role in the SNARE complex vesicle-membrane zippering and fusion mechanism (Sutton et al. 1998; Washbourne et al. 2002; Sudhof 2004).

Here we provide the first biological link that shows that miR-128 regulates *SNAP-25* and *Syt1* mRNAs, and we also show that the downregulation of this miRNA increases the expression levels of SNAP-25 and Syt1 proteins in neurons in culture, which places miR-128 as a possible functional regulator of synaptic transmission.

Examination of the effect of AD progression on miR-128 levels in the hippocampus of 5xFAD mice model revealed downregulation of miR-128 levels in 8 months of age mice compared to control littermates, but not at 2 or 12 months of age. Kimura and Ohno (2009) showed in their study that under the age of 4 months, there is no reduction in neuronal activity in the hippocampus of 5xFAD mice compared to WT mice. They also found that impaired synaptic activity was recorded starting from the age of 6 months (Oddo et al. 2006; Kimura and Ohno 2009; Kimura et al. 2010). Combining our results with the findings of Kimura and Ohno brings us to assume that at 2 months of age, although there is already intraneural Aβ accumulation in mice and initial deposition in the subiculum (Oakley et al. 2006), these accumulations do not lead to detrimental effects on synaptic activity yet, and also, there is no effect on miR-128 expression. At 8 months of age, there is intra and extracellular heavy Aβ plaques burden, which already significantly attenuates synaptic activity (Kimura and Ohno 2009). In this pathological condition, the expression level of miR-128 is being significantly downregulated. Interestingly, at 12 months of age, when there is massive synaptic degeneration and significant neuronal loss in 5xFAD model (Oakley et al. 2006; Eimer and Vassar 2013), the differenses in miR-128 expression compared to WT littermates are diminished. We speculate

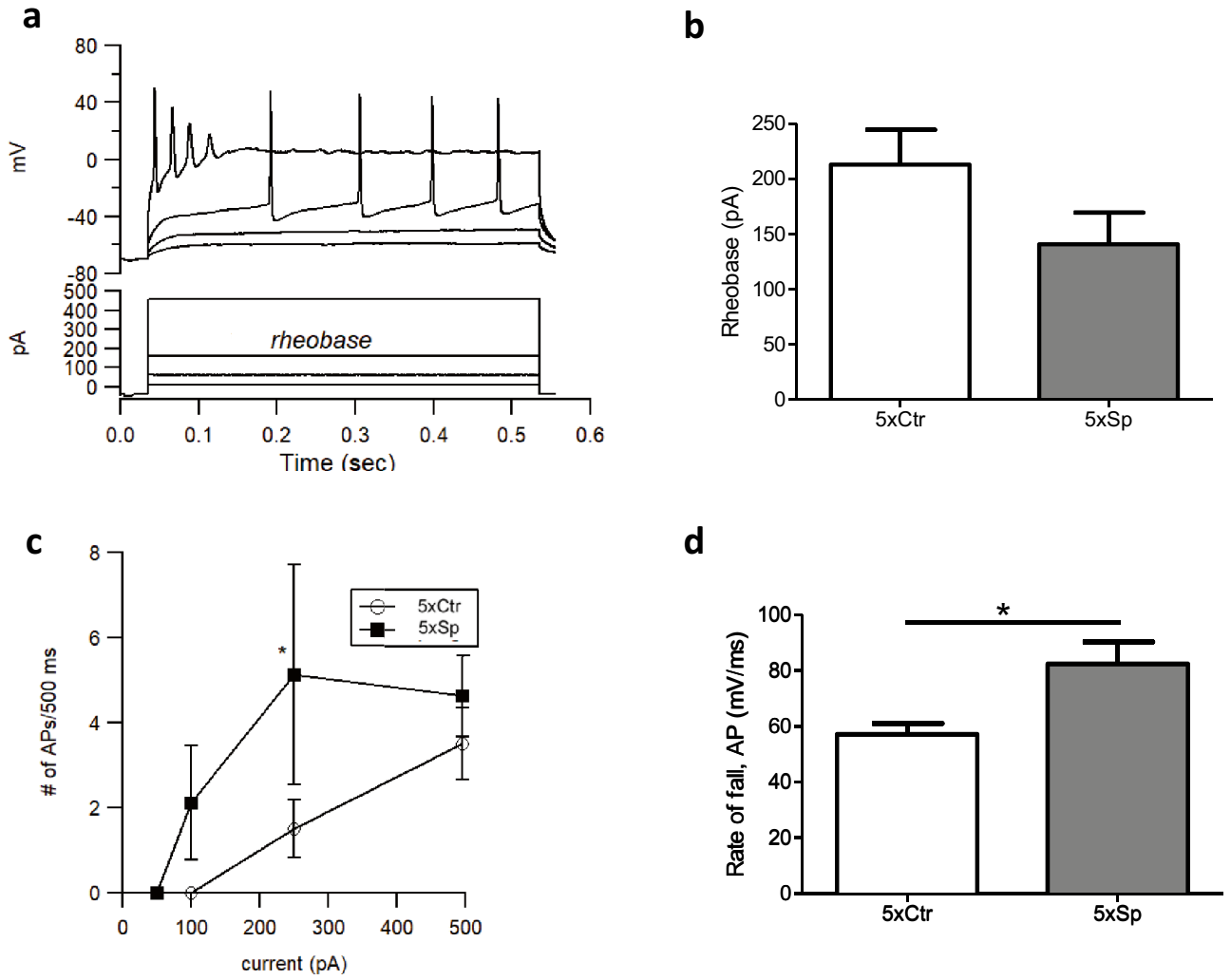


**Fig. 4** Electrophysiological recordings from 5xFAD primary hippocampal neurons expressing miR128-Sp or its control shows that miR-128 downregulation alters intrinsic neuronal excitability. 5xFAD hippocampal primary neuronal cultures were infected with miR128-Sp (5xSp) or with a control construct missing the active sponge sequence (5xCtr). **a** An example of voltage traces in response to increasing depolarization in 5xFAD hippocampal neuron infected with miR128-Sp. **b** Neurons infected with miR128-Sp show a trend of reduced rheobase levels compared to control cultures, meaning that lower current is required to evoke an action potential ($p < 0.5$). **c** The number of action potentials evoked in a certain current was higher in miR128-Sp infected cultures compared to their control. **d** The rate of falling phase of the action potentials in neurons with reduced levels of miR-128 (5xSp group) was faster than in control neurons (5xCtr group). The results are presented as mean + SEM ($n = 6–8$). Statistical significance was assessed by Student's unpaired *t*-test. *$p < 0.05$

that the role of miR-128 in AD might be abolished in a chronic stage of AD when there is a wide scale neuronal damage.

Environmental enrichment stimulates neuronal plasticity and synaptic transmission, as opposed to the neurodegenerative processes that happen with AD pathology's progression. EE was shown in many studies to improve cognition (Nilsson et al. 1999; Van Praag 2008; Vivar et al. 2012; Mustroph et al. 2012) and is known to partially mitigate AD pathology (Jankowsky et al. 2003, 2005; Lazarov et al. 2005; Costa et al. 2007; Dong et al., 2007; Laviola et al. 2008; Herring et al. 2009). Some of these mitigating effects have been recently associated with miRNA regulation (Barak et al. 2013; Shen et al. 2019; Wei et al. 2020; Nakano et al. 2020). Studying the effect of EE on miR-128 expression in 8-month-old WT and 5xFAD mice revealed that miR-128 was downregulated in WT but not in 5xFAD mice. The lack of changes in miR-128 expression levels in 5xFAD following EE is consistent with the findings published by Hüttenrauch et al. (2017), suggesting that EE does not improve behavioral performances or AD pathology–related phenotypes in 12-month-old 5xFAD mice despite prolonged (11 months) exposure to EE. This might be due to the high severity of this model which can hardly be alleviated by EE. Another

possibility is that EE fails to cause further downregulation in the levels of miR-128 due to its already decreased levels in the hippocampus of 8-month-old 5xFAD mice.

Interestingly, the direction of the alteration in miR-128 expression in WT mice following EE is the same as in 5xFAD 8-month-old mice and in individuals with AD (Lau et al. 2013). Combining these findings with our revelation that miR-128 regulates SNAP-25 and Syt1 proteins expression, known to be essential for synaptic transmission, we proposed that miR-128 downregulation in AD might play a compensatory role in the molecular mechanism that leads to increased synaptic transmission and cognitive enhancement. We speculate that miR-128 downregulation in AD may be related to compensatory mechanisms activated in AD which are similar to mechanisms of cognitive enhancement following EE.

Neuronal compensation is a mechanism that is assumed to be accountable for functional reservation or mitigation of cognitive or motor dysfunction due to the neuronal deterioration as a result of pathology progression (Barulli and Stern 2013; Scheller et al. 2014; Gregory et al. 2017). Compensation may be represented by increased activation of existing networks (Barulli and Stern 2013) or by recruitment of regions unrelated to a certain task that enable the performance of a function (Stern 2006). The enhancement in neuronal activity that we detected in this study might represent one of these mechanisms.

One of the factors that are strongly related to cognitive deterioration in AD is impaired synaptic transmission due to reduced levels of synaptic proteins and synaptic loss (Yao et al. 2003; Murphy et al. 2003; Kennedy et al. 2005). Among the revealed downregulated synaptic transmission–related proteins are pre-synaptic membrane proteins such as SNAP-25 and syntaxin (Sze et al. 1997, 2000) that are involved in vesicle docking and fusion and pre-synaptic vesicle proteins such as Syt1 and synaptophysin (Counts et al. 2006; Sze et al. 1997) that are essential for vesicular fusion and exocytosis. The downregulation of these proteins can lead to synaptic dysfunction and degeneration. Interestingly, several studies showed that as part of a compensatory mechanism, there is a significant increase in the size and the number of the contacts of the remaining synapses in neocortical and hippocampal regions of AD patients as the number of the synapses declines in a given region, as an attempt to increase the functioning efficiency of the remaining synapses (Scheff et al. 1990, 2006; DeKosky and Scheff 1990; Bertoni-Freddari et al. 1990).

Considering the proposed assumption of compensation, it is possible that miR-128 levels in the hippocampus of 5xFAD mice, at the age of 8 months, are significantly downregulated as part of a compensatory mechanism, allowing the upregulation of proteins that are essential for synaptic transmission (SNAP-25 and Syt1) to boost the neuronal functioning and recompense the reduction in synaptic activity. At 12 months of age, there is wide-scale neuronal damage in 5xFAD mice accompanied by neuronal death, and therefore at this pathological stage, possibly, the compensatory mechanisms are not effective, and this can be the reason for less significant downregulation of miR-128 in this age. However, to establish the compensatory role of miR-128 in AD, further experiments are required.

Interestingly, although Lau et al. (2013) also demonstrated a downregulation of miR-128 expression in the hippocampal area of individuals with AD, no significant alteration in miR-128 expression was found in the pre-frontal cortex of human subjects with AD pathology. In future work, it will be of high interest to investigate if miR-128 expression is being affected in other brain areas in AD and following EE.

The interaction of SNAP-25 with Syt1 proteins controls synaptic vesicular docking, priming, and fusion and is the key player in calcium triggered synchronous synaptic exocytosis (Geppert et al. 1994; Sørensen et al. 2002; Mohrmann et al. 2013). Also, Mohrmann et al. (2013) showed that the combination of these two proteins governs the vesicles releasable pool. These facts, combined with our findings showing that downregulation of miR-128 results in increased expression of SNAP-25 and Syt1 proteins, correlate with our measurements of increased neuronal activity in 5xFAD primary hippocampal cultures as a response to miR-128 downregulation.

These results are in line with the research performed in mice cortical primary neurons and used microelectrode array (MEA) to evaluate the effect of miR-128 inhibition on neuronal network activity (McSweeney et al. 2016). This study showed that reduction of miR-128 levels in neurons causes a significant elevation in neuronal activity.

Additionally, increased neuronal excitability may also contribute to an increased neuronal activity following miR-128 downregulation in hippocampal neurons. Whole-cell patch-clamp recordings from 5xFAD hippocampal primary neurons revealed that indeed, neurons with downregulated levels of miR-128 presented higher excitability in comparison to control neurons and also presented changes in the shape of the action potential. These findings suggest that in addition to the effect of increased levels of SNAP-25 and Syt1 on neuronal activity following the reduction of miR-128, there might be an additional effect of this miRNA on neuronal excitability through regulation of sodium and potassium voltage-gated ion channels that regulate the frequency and shape of the action potential.

## Conclusions

For the first time to date, we established a functional connection between miR-128 and two central proteins in synaptic transmission machinery: SNAP-25 and Syt1. We showed

that the downregulation of this miRNA increases synaptic excitability and neuronal network activity in 5xFAD neuronal cultures. We found that miR-128 is downregulated both following AD pathology and also following exposure of mice to an enriched environment. Taking all the findings together, we propose that miR-128 may possibly play a compensatory role in synapses that are deregulated with the progression of AD pathology. Altogether, the study presented here places the miR-128 as a synaptic player and opens a new direction for further research of the role of miR-128 in AD.

**Acknowledgements** We would also like to thank the members of the Ph.D. committee of Dr. Inna Shvarts-Serebro, Prof. Frenkel Dan, and Prof. Hornstein Eran for their meaningful comments, guidance, and recommendations.

**Author Contribution** Inna Shvarts-Serebro is a principal author. She designed the research, conducted the experiments, collected and analyzed the data, and wrote the manuscript. Anton Sheinin performed the patch clamp experiment and analyzed its data. Irit Gottfried advised the methodology and experimental design and assisted in the molecular biology and imaging technical part. Lior Adler assisted in primary neuron culturing and neuronal culture treatment. Nofar Schottlender was involved in some of the staining experiments. Uri Ashery is the supervisor of the research. Uri Ashery and Boaz Barak advised the research design and methodology, problem solving, result interpretation, and manuscript review.

**Funding** This work was supported by Israel Science Foundation (ISF grants 953/16 and 2141/20) and the DFG (NA: 207/10–1) to UA.

## Declarations

**Ethics Approval** All experimental procedures were approved by the Tel-Aviv University Animal Care Committee (approval 04–17-026), in accordance with the regulations and guidelines of Israel National Institute of Health and the US NIH Guidelines for the Care and Use of Laboratory Animals.

**Conflict of Interest** The authors declare no competing interests.

## References

Ashery U, Bielopolski N, Lavi A, Barak B, Michaeli L, Ben-Simon Y, Sheinin A, Bar-On D, Shapira Z. and Gottfried I (2014) The molecular mechanisms underlying synaptic transmission: a view of the presynaptic terminal. In The synapse pp. 21–109. Academic Press

Balthazar J, Schöwe NM, Cipolli GC et al (2018) Enriched environment significantly reduced senile plaques in a transgenic mice model of Alzheimer's disease, improving memory. Front Aging Neurosci 10:288. https://doi.org/10.3389/fnagi.2018.00288

Barak B, Shvarts-Serebro I, Modai S et al (2013) Opposing actions of environmental enrichment and Alzheimer's disease on the expression of hippocampal microRNAs in mouse models. Transl Psychiatry 3(10):1038–1077. https://doi.org/10.1038/tp.2013.77

Bartel DP (2004) MicroRNAs: genomics, biogenesis, mechanism, and function. Cell 116(2):281–297

Barulli D, Stern Y (2013) Efficiency, capacity, compensation, maintenance, plasticity: emerging concepts in cognitive reserve. Trends Cogn Sci 17:502–509

Beauquis J, Pavía P, Pomilio C et al (2013) Environmental enrichment prevents astroglial pathological changes in the hippocampus of APP transgenic mice, model of Alzheimer's disease. Exp Neurol 239:28–37. https://doi.org/10.1016/j.expneurol.2012.09.009

Bertoni-Freddari C, Fattoretti P, Casoli T, Meier-Ruge W, Ulrich J (1990) Morphological adaptive response of the synaptic junctional zones in the human dentate gyrus during aging and Alzheimer's disease. Brain Res 517:69–75

Brose N, Petrenko AG, Südhof TC, Jahn R (1992) Synaptotagmin: a calcium sensor on the synaptic vesicle surface. Science 256:1021–1025

Brunger AT, Choi UB, Lai Y et al (2019) The pre-synaptic fusion machinery. Curr Opin Struct Biol 54:179–188

Bushati N, Cohen SM (2008) MicroRNAs in neurodegeneration. Curr Opin Neurobiol 18(3):292–296

Chodzko-Zajko WJ, Schuler P, Solomon J, Heinl B, Ellis NR (1992) The influence of physical fitness on automatic and effortful memory changes in aging. Int J Aging Hum Dev 35:265–285

Choi UB et al (2010) Single-molecule FRET-derived model of the synaptotagmin 1–SNARE fusion complex. Nat Struct Mol Biol 17:318–324

Costa DA, Cracchiolo JR, Bachstetter AD, Hughes TF, Bales KR, Paul SM, Mervis RF, Arendash GW, Potter H (2007) Enrichment improves cognition in AD mice by amyloid-related and unrelated mechanisms. Neurobiol Aging 28(6):831–844

Counts SE, Nadeem M, Lad SP, Wuu J, Mufson EJ (2006) Differential expression of synaptic proteins in the frontal and temporal cortex of elderly subjects with mild cognitive impairment. J Neuropathol Exp Neurol 65(6):592–601

Cracchiolo JR, Mori T, Nazian SJ, Tan J, Potter H, Arendash GW (2007) Enhanced cognitive activity–over and above social or physical activity–is required to protect Alzheimer's mice against cognitive impairment, reduce Aβdeposition, and increase synaptic immunoreactivity. Neurobiol Learn Mem 88:277–294

Dandi E, Kalamari A, Touloumi O, Lagoudaki R, Nousiopoulou E, Simeonidou C, Spandou E, Tata DA (2018) Beneficial effects of environmental enrichment on behavior, stress reactivity and synaptophysin/BDNF expression in hippocampus following early life stress. Int J Dev Neurosci 1(67):19–32

Davis TH, Cuellar TL, Koch SM, Barker AJ, Harfe BD, McManus MT, Ullian EM (2008) Conditional loss of Dicer disrupts cellular and tissue morphogenesis in the cortex and hippocampus. J Neurosci 28:4322–4330

DeKosky ST, Scheff SW (1990) Synapse loss in frontal cortex biopsies in Alzheimer's disease: correlation with cognitive severity. Ann Neurol 27(5):457–464

Dong S, Li C et al (2007) Environment enrichment rescues the neurodegenerative phenotypes in presenilins-deficient mice. Eur J Neurosci 26(1):101–112

Eimer WA, Vassar R (2013) Neuron loss in the 5XFAD mouse model of Alzheimer's disease correlates with intraneuronal Aβ42 accumulation and Caspase-3 activation. Mol Neurodegener 8:2

Eriksen JL, Janus CG (2007) Plaques, tangles, and memory loss in mouse models of neurodegeneration. Behav Genet 37:79–100

Eskes GA, Longman S et al (2010) Contribution of physical fitness, cerebrovascular reserve and cognitive stimulation to cognitive function in post-menopausal women. Front Aging Neurosci 2:137

Frick KM, Fernandez SM (2003) Enrichment enhances spatial memory and increases synaptophysin levels in aged female mice. Neurobiol Aging 24(4):615–626

Geppert M, Goda Y, Hammer RE et al (1994) Synaptotagmin I: A major $Ca^{2+}$ sensor for transmitter release at a central synapse. Cell 79:717–727. https://doi.org/10.1016/0092-8674(94)90556-8

Gregory S, Long JD, Klöppel S et al (2017) Operationalizing compensation over time in neurodegenerative disease. Brain 140:1158–1165. https://doi.org/10.1093/brain/awx022

He M, Liu Y et al (2012) Cell-type-based analysis of microRNA profiles in the mouse brain. Neuron 73(1):35–48

Herring A, Ambrée O, Tomm M, Habermann H, Sachser N, Paulus W, Keyvani K (2009) Environmental enrichment enhances cellular plasticity in transgenic mice with Alzheimer-like pathology. Exp Neurol 216(1):184–192

Hu Z, Li Z (2017) miRNAs in synapse development and synaptic plasticity. Curr Opin Neurobiol 45:24–31

Hüttenrauch M, Walter S, Kaufmann M, WeggenS WO et al (2017) Limited effects of prolonged environmental enrichment on the pathology of 5XFAD mice. Mol Neurobiol 54(8):6542–6555

Improta-Caria AC, Nonaka CK, Cavalcante BR, De Sousa RA, Aras Júnior R, Souza BS (2020) Modulation of microRNAs as a potential molecular mechanism involved in the beneficial actions of physical exercise in Alzheimer disease. Int J Mol Sci 21(14):4977. https://doi.org/10.3390/ijms21144977

Irvine K, Laws KR, Gale TM, Kondel TK (2012) Greater cognitive deterioration in women than men with Alzheimer's disease: a meta analysis. J Clin Exp Neuropsychol 34(9):989–998

Jankowsky JL, Xu G, Fromholt D, Gonzales V, Borchelt DR (2003) Environmental enrichment exacerbates amyloid plaque formation in a transgenic mouse model of Alzheimer disease. J Neuropathol Exp Neurol 62:1220–1227

Jankowsky JL, Melnikova T et al (2005) Environmental enrichment mitigates cognitive deficits in a mouse model of Alzheimer's disease. J Neurosci 25(21):5217–5224

Katz B, Miledi R (1970) Further study of the role of calcium in synaptic transmission. J Physiol 207(3):789–801

Kennedy MB, Beale HC, Carlisle HJ, Washburn LR (2005) Integration of biochemical signalling in spines. Nat Rev Neurosci 6(6):423–434

Kim J, Inoue K, Ishii J, Vanti WB, Voronov SV, Murchison E, Hannon G, Abeliovich A (2007) A microRNA feedback circuit in midbrain dopamine neurons. Science (new York, NY) 317:1220–1224

Kimura R, Ohno M (2009) Impairments in remote memory stabilization precede hippocampal synaptic and cognitive failures in 5XFAD Alzheimer mouse model. Neurobiol Dis 33:229–235

Kimura R, Devi L, Ohno M (2010) Partial reduction of BACE1 improves synaptic plasticity, recent and remote memories in Alzheimer's disease transgenic mice. J Neurochem 113:248–326

Lambert TJ, Fernandez SM et al (2005) Different types of environmental enrichment have discrepant effects on spatial memory and synaptophysin levels in female mice. Neurobiol Learn Mem 83(3):206–216

Lazarov O, Robinson J, Tang YP, Hairston IS, Korade-Mirnics Z, Lee VM, Hersh LB, Sapolsky RM, Mirnics K, Sisodia SS (2005) Environmental enrichment reduces Aβ levels and amyloid deposition in transgenic mice. Cell 120(5):701–713

Laviola G, Hannan AJ et al (2008) Effects of enriched environment on animal models of neurodegenerative diseases and psychiatric disorders. Neurobiol Dis 31(2):159–168

Lau P, Bossers K et al (2013) Alteration of the microRNA network during the progression of Alzheimer's disease. EMBO Mol Med 5(10):1613–1634

Lin Q, Wei W, Coelho CM, Li X, Baker-Andresen D, Dudley K, Ratnu VS, Boskovic Z, Kobor MS, Sun YE et al (2011) The brain-specific microRNA miR128b regulates the formation of fear-extinction memory. Nat Neurosci 14:1115–1117

Liu N, He S et al (2012) Early natural stimulation through environmental enrichment accelerates neuronal development in the mouse dentate gyrus. PLoS One 7(1):e30803

Ludwig N, Petra L et al (2016) Distribution of miRNA expression across human tissues. Nucleic Acids Res 44(8):3865–3877

Marchetti C, Marie H (2011) Hippocampal synaptic plasticity in Alzheimer's disease: what have we learned so far from transgenic models? Rev Neurosci 22(4):373–402

Masliah E, Crews L et al (2006) Synaptic remodeling during aging and in Alzheimer's disease. J Alzheimers Dis 9(3 Suppl):91–99

Mayeux R, Stern Y (2012) Epidemiology of Alzheimer disease. Cold Spring Harbor perspectives in medicine 2(8):a006239

McNeill E, Van Vactor D (2012) MicroRNAs shape the neuronal landscape. Neuron 75:363–379

Menkes-Caspi N, Yamin HG, Kellner V, Spires-Jones TL, Cohen D, Stern EA (2015) Pathological tau disrupts ongoing network activity. Neuron 5:959–966

McSweeney KM, Gussow AB et al (2016) Inhibition of microRNA 128 promotes excitability of cultured cortical neuronal networks. Genome Res 26:1411–1416

Mohrmann R, de Wit H, Connell E et al (2013) Synaptotagmin interaction with SNAP-25 governs vesicle docking, priming, and fusion triggering. J Neurosci 33:14417–14430. https://doi.org/10.1523/JNeurosci.1236-13.2013

Mouillet-Richard S, Baudry A, Launay JM, Kellermann O (2012) MicroRNAs and depression. Neurobiol Dis 46(2):272–278

Mohrmann R, Dhara M, Bruns D (2015) Complexins: small but capable. Cell Mol Life Sci 72:4221–4235

Murphy TH (2003) Activity-dependent synapse development: changing the rules. Nat Neurosci 6(1):9–11

Mustroph ML, Chen S, Desai SC et al (2012) Aerobic exercise is the critical variable in an enriched environment that increases hippocampal neurogenesis and water maze learning in male C57BL/6J mice. Neuroscience 219:62–71. https://doi.org/10.1016/j.neuroscience.2012.06.007

Nakano M, Kubota K, Hashizume S, et al (2020) An enriched environment prevents cognitive impairment in an Alzheimer's disease model by enhancing the secretion of exosomal microRNA-146a from the choroid plexusBrain, Behav Immun - Heal 9 100149 https://doi.org/10.1016/j.bbih.2020.100149

Nilsson M, Perfilieva E, Johansson U, Orwar O, Eriksson PS (1999) Enriched environment increases neurogenesis in the adult rat dentate gyrus and improves spatial memory. J Neurobiol 39(4):569–578

Nithianantharajah J, Levis H, Murphy M (2004) Environmental enrichment results in cortical and subcortical changes in levels of synaptophysin and PSD-95 proteins. Neurobiol Learn Mem 81(3):200–210

Oakley H, Cole SL, Logan S, Maus E, Shao P, Craft J, Guillozet-Bongaarts A, Ohno M, Disterhoft J, Eldik LV et al (2006) Intraneuronal β-amyloid aggregates, neurodegeneration, and neuron loss in transgenic mice with five familial Alzheimer's disease mutations: potential factors in amyloid plaque formation. J Neurosci 26:10129–10140

Oddo S, Caccamo A, Tran L, Lambert MP, Glabe CG, Klein WL, Frank M, LaFerla FM (2006) Temporal profile of amyloid-β (Aβ) oligomerization in an in vivo model of Alzheimer disease: a link between Aβ and tau pathology. J Biol Chem 281:1599–1604

Ohno M, Chang L, Tseng W, Oakley H, Citron M et al (2006) Temporal memory deficits in Alzheimer's mouse models: rescue by genetic deletion of BACE. Eur J Neurosci 23:251–260

Ohno M, Cole SL, Yasvoina M, Zhao J, Citron M, Berry R et al (2007) BACE1 gene deletion prevents neuron loss and memory deficits in 5XFAD APP/PS1 transgenic mice. Neurobiol Dis 26:134–145

Rampon C, Jiang CH, Dong H, Tang YP, Lockhart DJ, Schultz PG, Tsien JZ, Hu Y (2000) Effects of environmental enrichment on gene expression in the brain. Proc Natl Acad Sci 97(23):12880–12884

Rizo J, Xu J (2015) The synaptic vesicle release machinery. Annu Rev Biophys 44:339–367. https://doi.org/10.1146/annurev-biophys-060414-034057

Schaefer A, O'Carroll D, Tan CL, Hillman D, Sugimori M, Llinas R, Greengard P (2007) Cerebellar neurodegeneration in the absence of microRNAs. J Exp Med 204:553–1558

Schaie KW (1993) The Seattle Longitudinal Study: a thirty-five-year inquiry of adult intellectual development. Zeitschrift Fur Gerontologie 1(26):129–137

Scheff SW, DeKosky ST, Price DA (1990) Quantitative assessment of cortical synaptic density in Alzheimer's disease. Neurobiol Aging 11(1):29–37

Scheff SW, Price DA, Schmitt FA, Mufson EJ (2006) Hippocampal synaptic loss in early Alzheimer's disease and mild cognitive impairment. Neurobiol Aging 27(10):1372–1384

Scheller E, Minkova L, Leitner M, Klöppel S (2014) Attempted and successful compensation in preclinical and early manifest neurodegeneration — a review of task FMRI studies. Front Psychiatry 5:132

Selkoe DJ (2008) Soluble oligomers of the amyloid beta-protein impair synaptic plasticity and behavior. Behav Brain Res 192(1):106–113

Shankar GM, Walsh DM (2009) Alzheimer's disease: synaptic dysfunction and Aβ. Mol Neurodegener 4(1):1–3

Shao NY, Hu HY, Yan Z, Xu Y, Hu H, Menzel C, Li N, Chen W, Khaitovich P (2010) Comprehensive survey of human brain microRNA by deep sequencing. BMC Genomics 11(1):1–4

Shen J, Li Y, Qu C et al (2019) The enriched environment ameliorates chronic unpredictable mild stress-induced depressive-like behaviors and cognitive impairment by activating the SIRT1/miR-134 signaling pathway in hippocampus. J Affect Disord 248:81–90. https://doi.org/10.1016/j.jad.2019.01.031

Shomron N, Golan D et al (2009) An evolutionary perspective of animal microRNAs and their targets. J Biomed Biotechnol 594738

Shomron N, Levy C (2009) MicroRNA-biogenesis and Pre-mRNA splicing crosstalk. J Biomed Biotechnol 594678

Sørensen JB, Matti U, Wei SH et al (2002) The SNARE protein SNAP-25 is linked to fast calcium triggering of exocytosis. Proc Natl Acad Sci USA 99:1627–1632. https://doi.org/10.1073/pnas.251673298

Stern Y (2006) Cognitive reserve and Alzheimer disease. Alzheimer's Disease and Associated Disorders 20:112–117

Sudhof TC (2004) The Synaptic Vesicle Cycle Annu Rev Neurosci 27:509–547

Sutton RB, Fasshauer D, Jahn R, Brunger AT (1998) Crystal structure of a SNARE complex involved in synaptic exocytosis at 2.4 A resolution. Nature 395:347–353

Sze CI, Troncoso JC, Kawas C, Mouton P, Price DL, Martin LJ (1997) Loss of the presynaptic vesicle protein synaptophysin in hippocampus correlates with cognitive decline in Alzheimer disease. J Neuropathol Exp Neurol 56(8):933–944

Sze CI, Bi H et al (2000) Selective regional loss of exocytotic presynaptic vesicle proteins in Alzheimer's disease brains. J Neurol Sci 175(2):81–90

Tan CL, Plotkin J et al (2013) MicroRNA-128 governs neuronal excitability and motor behavior in mice. Science 342:1254–1258

Terry RD (2006) Alzheimer's disease and the aging brain. J Geriatr Psychiatry Neurol 19(3):125–128

Trinchese F, Liu S, Battaglia F, Walter S, Mathews PM, Arancio O (2004) Progressive age-related development of Alzheimer-like pathology in APP/PS1 mice. Annals of Neurology: Official J Am Neuro Assoc Child Neuro Soc 55(6):801–814

Van Praag H (2008) Neurogenesis and exercise: past and future directions. NeuroMol Med 10(2):128–140

Vergallo A, Lista S, Zhao Y et al (2021) MiRNA-15b and miRNA-125b are associated with regional Aβ-PET and FDG-PET uptake in cognitively normal individuals with subjective memory complaints. Transl Psychiatry 11:1–11. https://doi.org/10.1038/s41398-020-01184-8

Vivar C, Potter MC, van Praag H (2012) All about running: synaptic plasticity, growth factors and adult hippocampal neurogenesis. Curr Top Behav Neurosci 15:189–210. https://doi.org/10.1007/7854_2012_220

Wang WX, Huang Q, Hu Y, Stromberg AJ, Nelson PT (2011) Patterns of microRNA expression in normal and early Alzheimer's disease human temporal cortex: white matter versus gray matter. Acta Neuropathol 121:193–205

Wang S, Li Y, Ma C (2016) Synaptotagmin-1 C2B domain interacts simultaneously with SNAREs and membranes to promote membrane fusion. eLife 5:209–217

Washbourne P, Thompson PM, Carta M, Costa ET, Mathews JR, Lopez-Bendito G, Molnar Z, Becher MW, Valenzuela CF, Partridge LD, Wilson MC (2002) Genetic ablation of the t-SNARE SNAP-25 distinguishes mechanisms of neuroexocytosis. Nat Neurosci 5:19–26

Wei Z, Meng X, Fatimy El R et al (2020) Environmental enrichment prevents Aβ oligomer-induced synaptic dysfunction through mirna-132 and hdac3 signaling pathways Neurobiol Dis 134:104617 https://doi.org/10.1016/j.nbd.2019.104617

Wolf SA, Kronenberg G, Lehmann K, Blankenship A, Overall R, Staufenbiel M, Kempermann G (2006) Cognitive and physical activity differently modulate disease progression in the amyloid precursor protein (APP)-23 model of Alzheimer's disease. Biol Psychiatry 60:1314–1323

Wong HK,Veremeyko T, Patel N, Lemere CA, Walsh DM, Esau C, Vanderburg C, Krichevky AM (2013) De-repression of FOXO3a death axis by microRNA-132 and -212 causes neuronal apoptosis in Alzheimer's disease. Hum Mol Genet 22:3077–3092

Yao PJ, Zhu M, Pyun EI, Brooks AI, Therianos S, Meyers VE, Coleman PD (2003) Defects in expression of genes related to synaptic vesicle trafficking in frontal cortex of Alzheimer's disease. Neurobiol Dis 12(2):97–109

Zhou Q, Zhou P, Wang AL, Wu D, Zhao M, Südhof TC, Brunger AT (2017) The primed SNARE–complexin–synaptotagmin complex for neuronal exocytosis. Nature 548:420–425

Zovoilis A, Agbemenyah HY, Agis-Balboa RC, Stilling RM, Edbauer D, Rao P et al (2011) microRNA-34c is a novel target to treat dementias. EMBO J 30:4299–4308